Electronic Supplementary Material (ESI) for Soft Matter.
This journal is © The Royal Society of Chemistry 2016

Electronic Supplementary Information

Mesoporous self-assembled nanoparticles of biotransesterified cyclodextrins and nonlamellar lipids as carriers of water-insoluble substances

Leïla Zerkoune[1], Sylviane Lesieur[1], Jean-Luc Putaux[2,3], Luc Choisnard[4,5], Annabelle Gèze[4,5], Denis Wouessidjewe[4,5], Borislav Angelov[6], Corinne Vebert-Nardin[7], James Doutch[8], and Angelina Angelova[1,*]

[1] Institut Galien Paris-Sud, CNRS UMR 8612, Univ. Paris-Sud, Université Paris-Saclay, LabEx LERMIT, 5 rue J.-B. Clément, 92296 Châtenay-Malabry cedex, France,

[2] Université Grenoble Alpes, Centre de Recherches sur les Macromolécules Végétales (CERMAV), F-38000 Grenoble, France,

[3] CNRS, CERMAV, F-38000 Grenoble, France,

[4] Université Grenoble Alpes, Département de Pharmacologie Moléculaire (DPM), F-38000 Grenoble, France,

[5] CNRS UMR 5063, DPM, F-38000 Grenoble, France,

[6] Institute of Physics, ELI Beamlines, Academy of Sciences of the Czech Republic, Na Slovance 2, CZ-18221 Prague, Czech Republic,

[7] IPREM/EPCP, Technopole Helioparc, 2 Av. Pdt Angot, F-64053 PAU cedex 09, France,

[8] Diamond Light Source Ltd., Didcot, Oxfordshire, OX11 0DE, UK.

*Corresponding Author: Angelina.Angelova@u-psud.fr

I. Physico-chemical characteristics

Table S1. Physico-chemical properties of cyclodextrin nanocavities (from *Salústio et al.*, 2011).

	α-cyclodextrin	**β-cyclodextrin**	**γ-cyclodextrin**
Number of glucose units	6	7	8
Chemical formula	$C_{36}H_{60}O_{30}$	$C_{42}H_{70}O_{35}$	$C_{48}H_{80}O_{40}$
Molecular weight ($g.mol^{-1}$)	972	1135	1297
Solubility in water ($mol.L^{-1}$)	0.149	0.016	0.179
Ø nanocavity (Å)	5.7	7.8	9.5
Height of the macrocycle (Å)	7.9	7.9	7.9

Figure S1. Chemical structure of Oil red O (OR): 1-[2,5-Dimethyl-4-(2,5-dimethylphenylazo) phenylazo]-2-naphthol (MW 408.49).

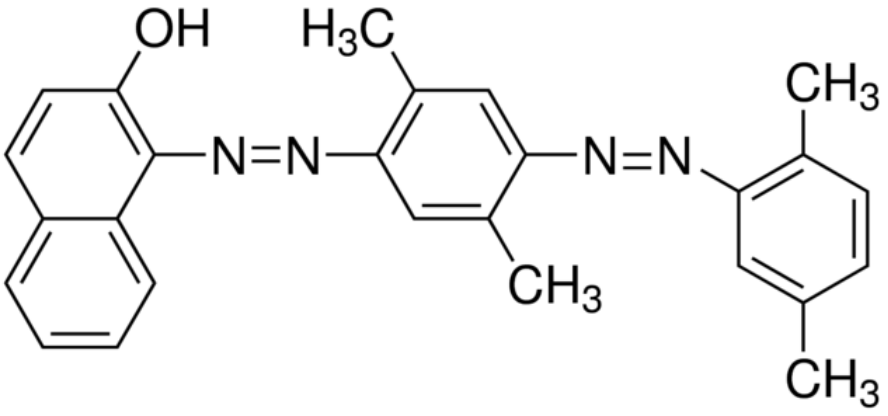

II. Additional results from from cross-polarised optical microscopy

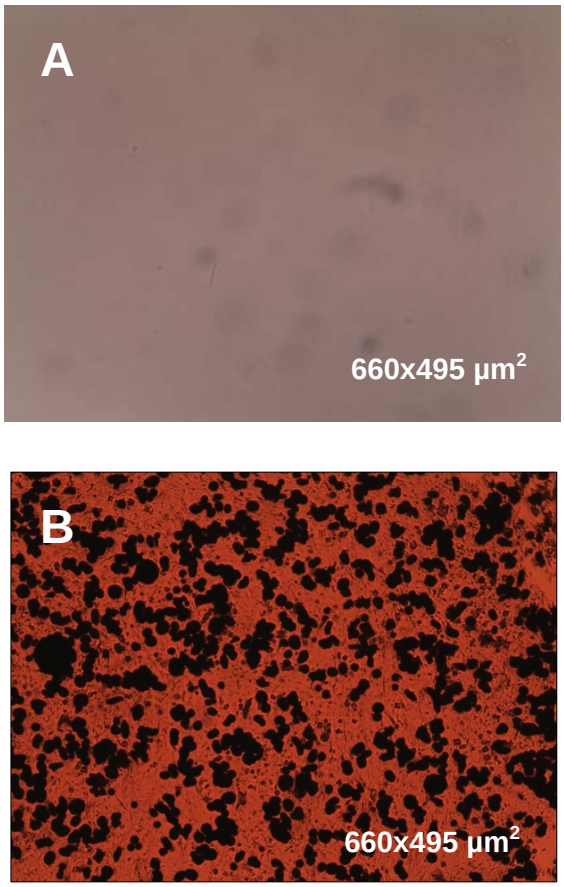

Figure S2. Cross-polarised optical microscopy (POM) images of liquid crystalline lipid membranes of monoolein (MO) containing 4 mol% βCD-nC_{10} (A). The sample was hydrated at 25 °C in 50 wt% aqueous phase without dispersion. The isotropic texture is typical for a cubic lattice organization of a MO-based assembly. Under the microscope, the image is viewed entirely black. (B) Nondispersed MO/P80/βCD-nC_{10} membranes (4 mol% βCD-nC_{10}) with added 15 mol% guest hydrophobic substance Oil red (OR) with regard to the lipid constituent MO. The dye OR partitions between its solubilized state in the bicontinuous cubic membrane and in domains of phase separated OR clusters. Image sizes: 660×495 µm^2. The magnification is ×10.

III. Additional results from quasi-elastic light scattering (QELS)

Figure S3. Nano-object hydrodynamic diameter measurements by quasi-elastic light scattering presented as intensity and volume distribution plots for self-assembled MO/P80 and MO/P80/β-CD-nC_{10} nanocarriers (4 mol% βCD-nC_{10} deep cavitand content) produced through dispersion by 15 mol.% P80 surfactant additive with respect to the nonlamellar lipid MO: (Black plots) MO/15 mol% P80 assemblies; (Red plots) MO/15 mol% P80/4 mol% βCD-C_{10} assemblies. Aqueous phase: Milli Q water. Temperature is 25°C.

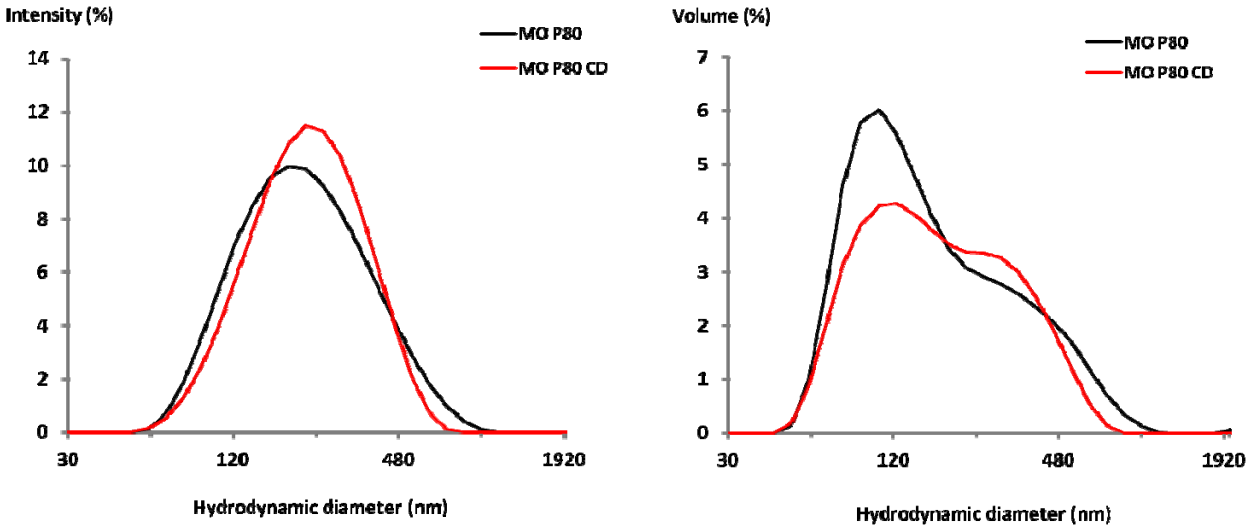

Figure S4. Determination of nano-object populations and hydrodynamic diameters [nm] through a multimodal model analysis of quasi-elastic light scattering data of self-assembled MO/P80 nanocarriers obtained upon lipid film dispersion in the presence of variable quantities of surfactant stabilizer with respect to the nonlamellar lipid MO: (a) 5 mol.% P80; (b) 10 mol.% P80; and (c) 15 mol.% P80. Aqueous phase: Milli Q water. Temperature is 25°C.

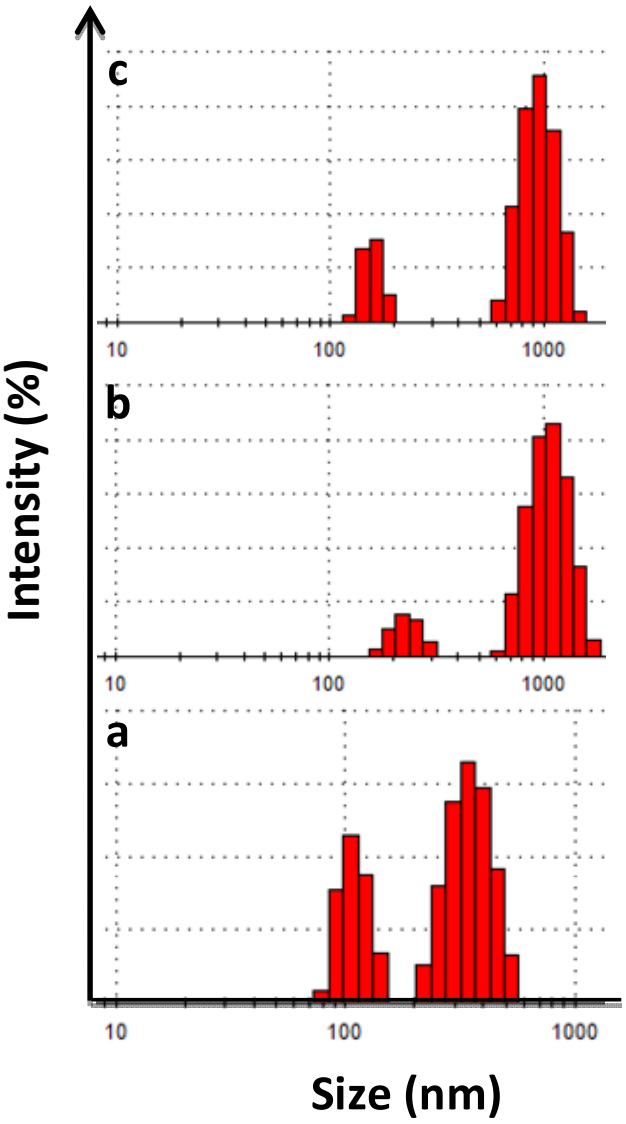

Figure S5. Determination of nano-object populations and hydrodynamic diameters [nm] through a multimodal model analysis of quasi-elastic light scattering data of self-assembled MO/P80/β-CD-nC_{10} nanocarriers (4 mol% βCD-nC_{10} deep cavitand content) produced upon dispersion of a mixed amphiphilic film in the presence of variable quantities of surfactant stabilizer with respect to the nonlamellar lipid MO: (a') 5 mol.% P80; (b') 10 mol.% P80; and (c') 15 mol.% P80. Aqueous phase: Milli Q water. Temperature is 25°C.

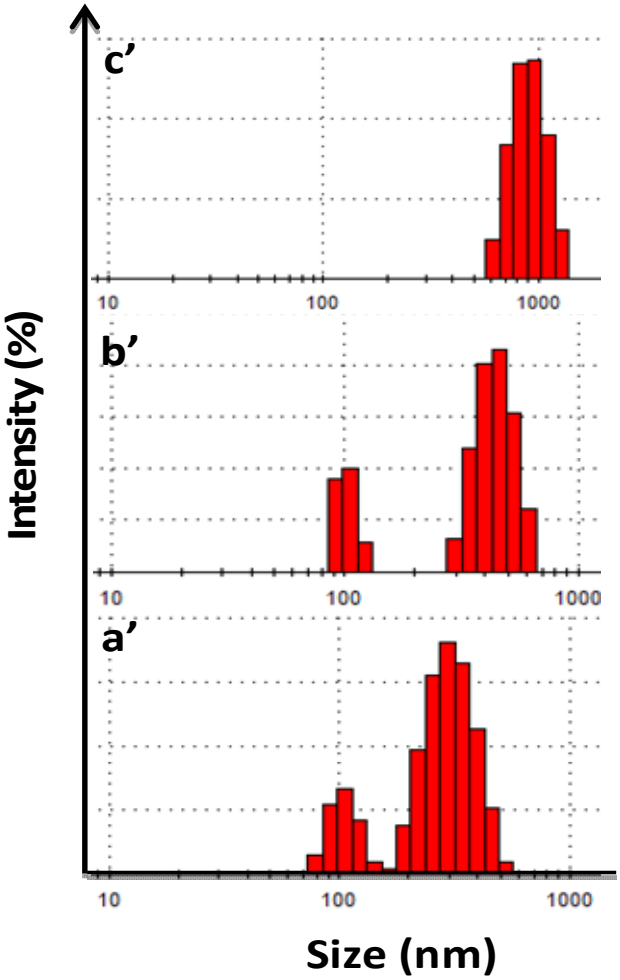

Figure S6. Nano-object hydrodynamic diameter measurements by quasi-elastic light scattering presented as intensity and volume distribution plots for self-assembled MO/5 mol% P80 and MO/5 mol% P80/β-CD-nC_{10} nanocarriers (4 mol% βCD-nC_{10} deep cavitand content) encapsulating variable quantities of hydrophobic guest substance Oil red: 0 mol% (black plots), 0.5 mol% (red plots), 1 mol% (blue plots), 1.5 mol% (purple plots) and 2 mol% OR dye (green plots). Aqueous phase: Milli Q water. Temperature is 25°C.

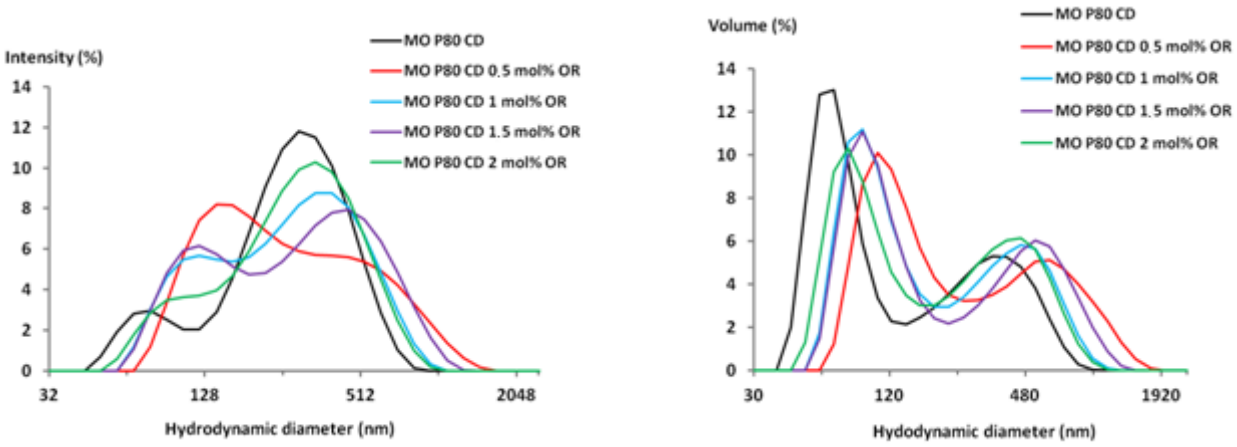

Figure S7. Determination of nano-object populations and hydrodynamic diameters [nm] through a multimodal model analysis of quasi-elastic light scattering data of self-assembled MO/5 mol% P80/OR nanocarriers produced upon dispersion of a mixed amphiphilic film encapsulating (a) 0 mol%; (b) 0.5 mol%; (c) 1 mol%; (d) 1.5 mol%, and (e) 2 mol% guest OR dye with respect to the lipid MO. Aqueous phase: Milli Q water. Temperature is 25°C.

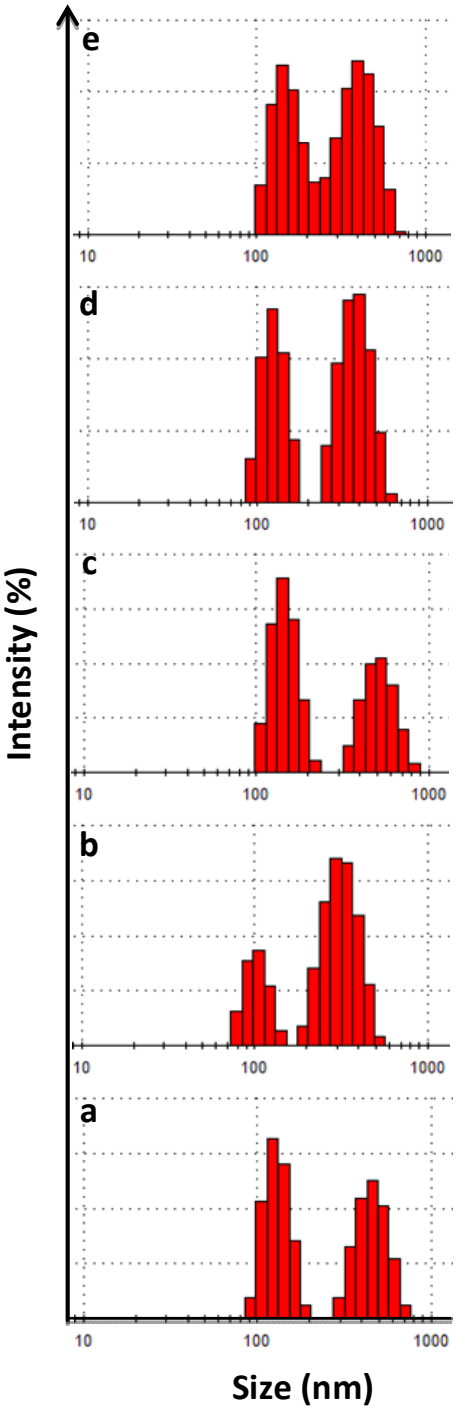

Figure S8. Determination of nano-object populations and hydrodynamic diameters [nm] through a multimodal model analysis of quasi-elastic light scattering data of self-assembled MO/5 mol% P80/β-CD-nC_{10}/OR nanocarriers (4 mol% βCD-nC_{10} deep cavitand content) produced upon dispersion of a mixed film encapsulating (a) 0 mol%; (b) 0.5 mol%; (c) 1 mol%; (d) 1.5 mol%, and (e) 2 mol% guest OR dye with respect to the lipid MO. Aqueous phase: Milli Q water. Temperature is 25°C.

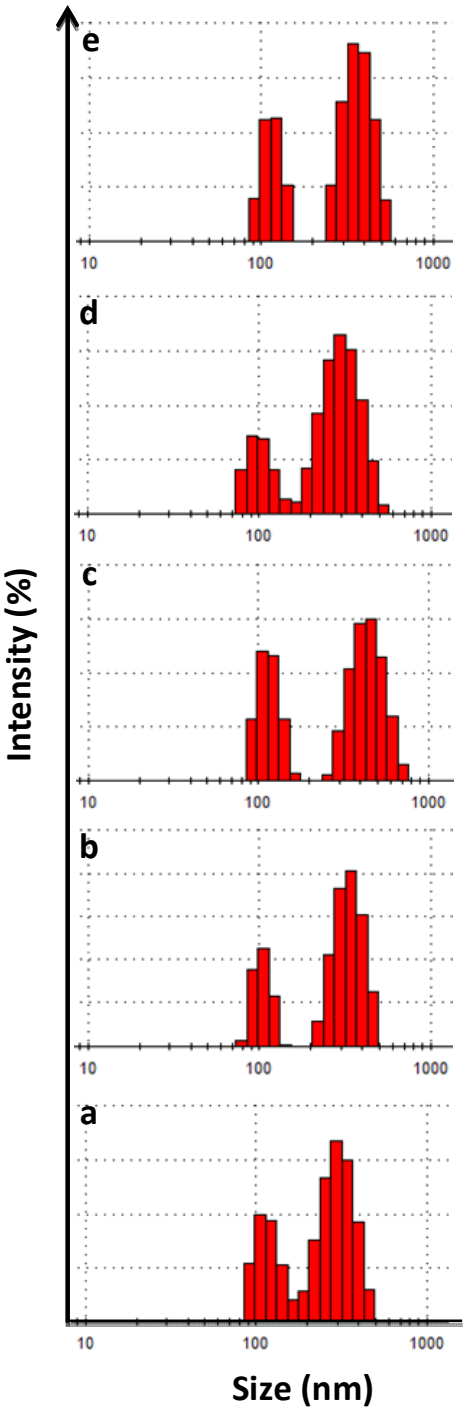

IV. Additional results from UV-Visible spectroscopy and optical density measurements

Figure S9. (Top) Optical density *versus* concentration curves of oil red (OR) dissolved in ethanol solvent. (Bottom) Standard plot for determination of the molar extinction coefficient of OR (ε=26994 L.mol^{-1}.cm^{-1}) at λ_{max} = 516 nm.

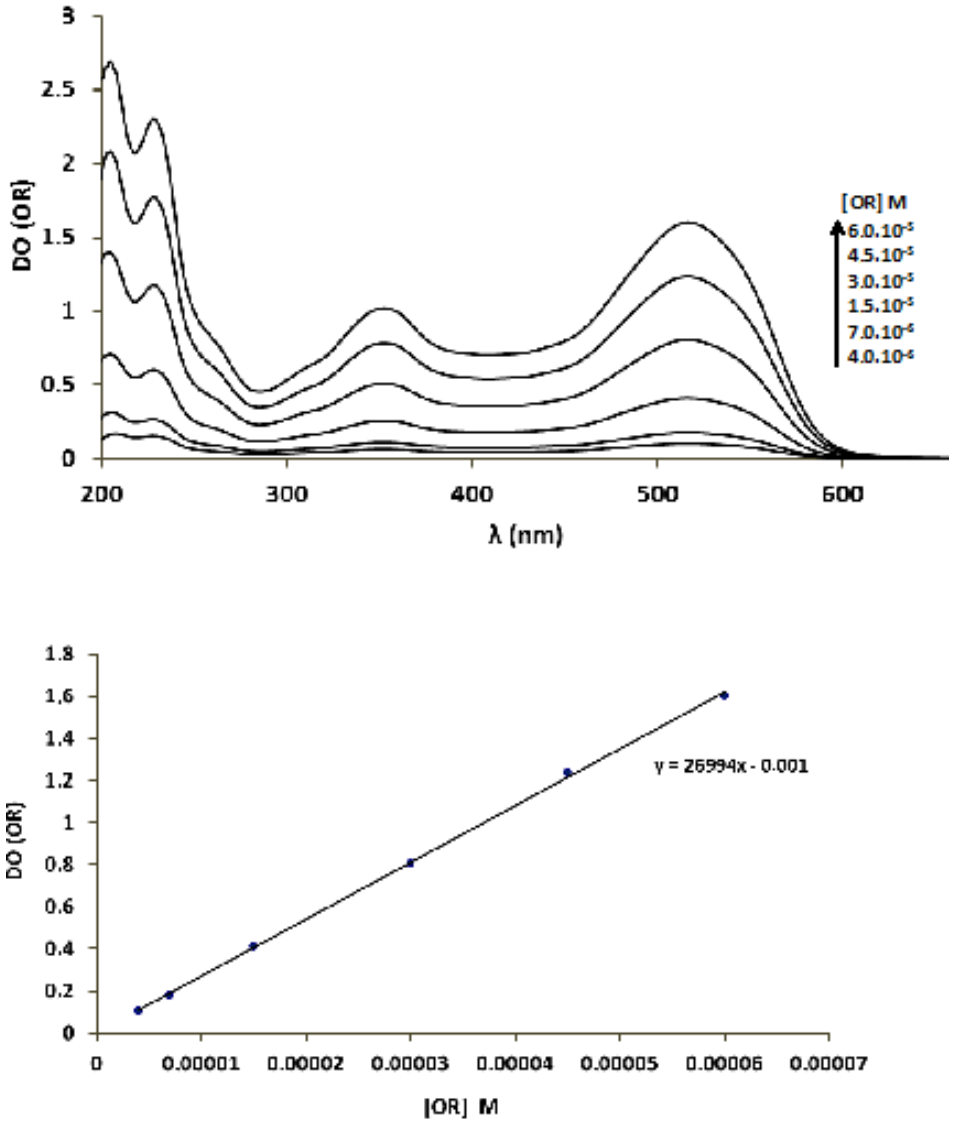

Figure S10. UV-Vis spectra of OR measured after dissolution of the nanocarrier formulations (100 µL) in ethanol solvent. The MO/P80 and MO/P80/βCD-nC_{10} carriers were studied at different OR loadings and $[OR]_{nano}$ was defined as the concentration of nanoencapsulated OR in the aqueous dispersions of nanocarriers. Standard calibration plot (absorbance *versus* OR concentration) was used for quantification of the nanoencapsulated OR in MO/P80 and MO/P80/βCD-nC_{10} prepared from mixed films containing 0.5, 1.0, 1.5 and 2 mol% OR with respect to the nonlamellar lipid MO. Temperature is 25 °C.

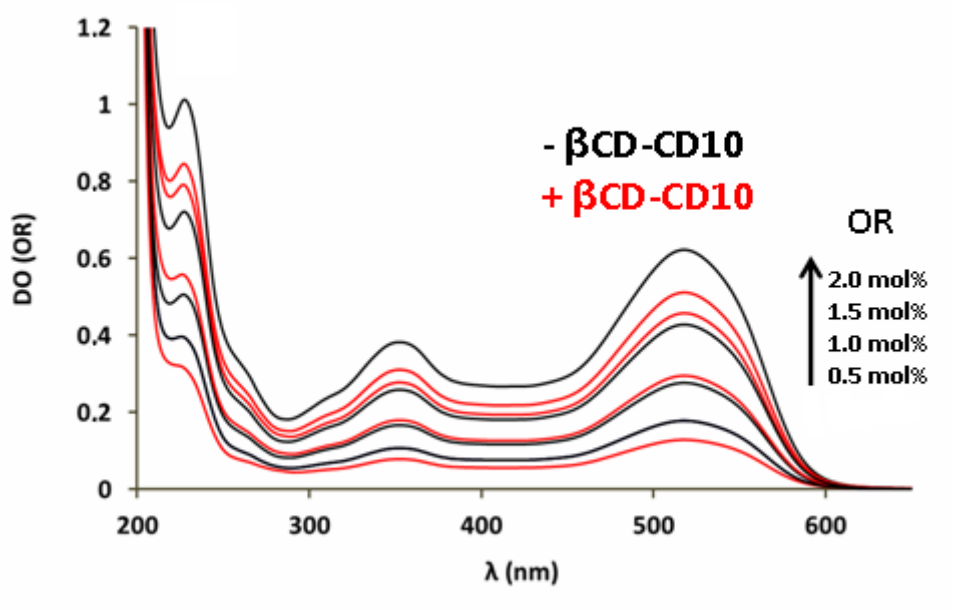

Figure S11. Encapsulation efficiency of Oil red (OR) in MO/5 mol% P80 assemblies (dark grey plots) and in MO/5 mol% P80/β-CD-nC_{10}/OR nanocarriers (at 4 mol% βCD-nC_{10} deep cavitand content) (light grey plots) *versus* the molar percentage of the model nanodrug OR. The corresponding analytical determinations of the optical densities were done at a wavelength λ = 524 nm using standard curves OD *versus* OR concentration. The molar percentages of OR were calculated as [number of moles of OR]×100 / [total number of moles of substances present in the amphiphilic system] (%).

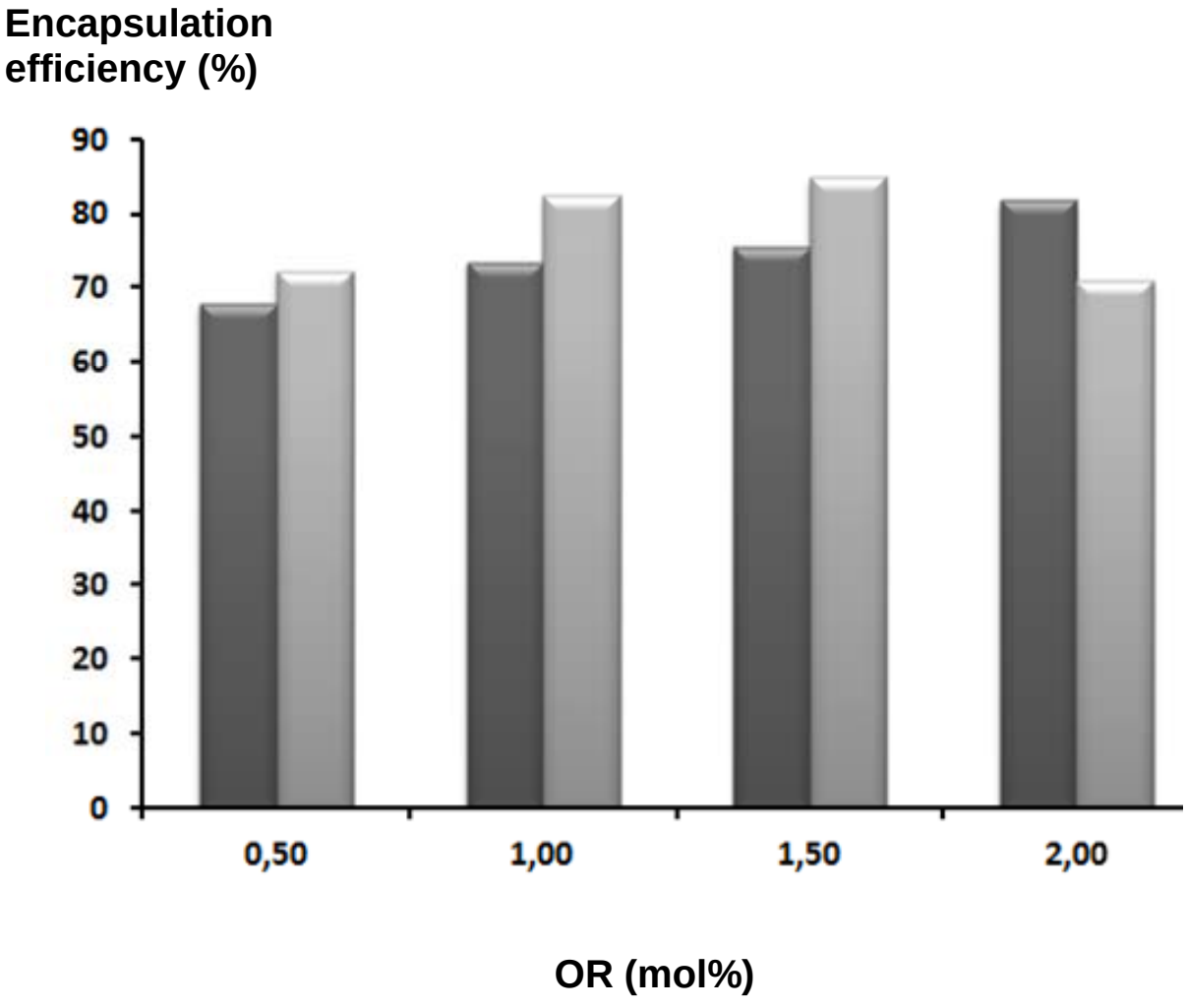

V. References

1. P. J. Salústio, P. Pontes, C. Conduto, I. Sanches, C. Carvalho, J. Arrais, M. Cabral and M. H. Marques, *Pharm Sci.Tech*., 2011, **12**, 1276-1292.
2. Gulik, A., Delacroix, H., Wouessidjewe, D., and Skiba, M. *Langmuir* 1998, **14**, 1050-1057.
3. L. Boulmedarat, G. Piel, A. Bochot, S. Lesieur, L. Delattre and E. Fattal, *Pharm. Research*, 2005, **22**, 962-971.
4. D. Duchene, G. Ponchel and D. Wouessidjewe, *Adv. Drug Deliv. Rev.*, 1999, **36**, 29–40.
5. E. Lemos-Senna, D. Wouessidjewe, D. Duchêne and S. Lesieur, *Colloids and Surfaces B: Biointerfaces,* 1998, **10**, 291-301.
6. S. Lesieur, D. Charon, P. Lesieur, C. Ringard-Lefebvre, V. Muguet, D. Duchêne and D. Wouessidjewe, *Chem. Phys. Lipids*, 2000, **106**, 127-144.
7. C. Gervaise, V. Bonnet, O. Wattraint, F. Aubry, C. Sarazin, P.A. Jaffrès and F. Djedaïni-Pilard, *Biochimie,* 2012, **94**, 66–74.
8. B. Angelov, M. Ollivon and A. Angelova, *Langmuir*, 1999, **15**, 8225-8234.
9. J. N. Israelachvili, D. J. Mitchell and B. W. Ninham, *Journal of the Chemical Society, Faraday Transactions 2: Molecular and Chemical Physics*, 1975, **72**, 1525-1550.
10. R.A. Karjibana, M. Basria, M.B.A. Rahmana and A.B Salleh, *APCBEE Procedia*, 2012, **3**, 287-297.
11. J. Dubochet, M. Adrian, J. J.Chang, J. C. Homo, J. Lepault, A.W. McDowall and P. Schultz, *Q Rev Biophys*., 1988, **21**, 129-228.
12. J. Kuntsche, J.C. Horst, H. Bunjes, *International Journal of Pharmaceutics*, 2011, **417**, 120-137.